Fullerenes, Nanotubes and Carbon Nanostructures

ISSN: (Print) (Online) Journal homepage: https://www.tandfonline.com/loi/lfnn20

The effect of structure on the conductivity of disordered carbon (the case of graphene-containing shungite)

Igor Antonets, Yevgeny Golubev & Vladimir Shcheglov

To cite this article: Igor Antonets, Yevgeny Golubev & Vladimir Shcheglov (2023): The effect of structure on the conductivity of disordered carbon (the case of graphene-containing shungite), Fullerenes, Nanotubes and Carbon Nanostructures, DOI: 10.1080/1536383X.2023.2226273

To link to this article: https://doi.org/10.1080/1536383X.2023.2226273

Published online: 10 Jul 2023.

Submit your article to this journal

View related articles

View Crossmark data

Full Terms & Conditions of access and use can be found at
https://www.tandfonline.com/action/journalInformation?journalCode=lfnn20

FULLERENES, NANOTUBES AND CARBON NANOSTRUCTURES
https://doi.org/10.1080/1536383X.2023.2226273

Taylor & Francis
Taylor & Francis Group

Check for updates

The effect of structure on the conductivity of disordered carbon (the case of graphene-containing shungite)

Igor Antonets[a], Yevgeny Golubev[b], and Vladimir Shcheglov[c]

[a]Department of Radiophysics, Syktyvkar State University, Syktyvkar, Russia; [b]Institute of Geology of Komi SC, Russian Academy of Sciences, Syktyvkar, Russia; [c]Institute of Radio Engineering and Electronics, Russian Academy of Sciences, Moscow, Russia

ABSTRACT

Understanding the mechanisms of conductivity in disordered carbon materials is one key to creating applied materials based on them. We present a new promising approach to quantitatively assessing the effect of structural parameters on the conductivity of disordered sp^2 carbon materials within the framework of a simplified current tube model. Stacks of graphene layers of complex shape and chaotic in contacts as an aggregate of sequentially located and parallel tubes were presented. This approximation made it possible to obtain a reliable quantitative estimate of the influence of the stacks size of graphene layers and their size distribution, as well as the size of the gaps between the stacks on the conductivity. The theoretical positions of the model were tested using the experimentally obtained parameters of the structure of two typical natural disordered carbon materials (shungites).

ARTICLE HISTORY
Received 14 April 2023
Accepted 12 June 2023

KEYWORDS
Graphene-containing shungite carbon; disordered carbon; conductivity; electrical resistivity; current tubes model

1. Introduction

The electromagnetic properties of sp^2 carbon materials are widely used in modern industry and technology. The most demanded properties are the accumulation and storage of charge in electrochemical capacitors, shielding of electromagnetic radiation in a wide range of wavelengths.[1–8]

The electrical conductivity of carbon materials depends primarily on their chemical nature and structure.[9–13] A significant contribution to the conducting properties of dispersed carbon materials is made by the resistance of contacts of the dispersed phase, which depends both on the morphology of carbon particles (size, shape) and on the nature of the electrical contact between them. In addition, in porous carbon materials, there is additional resistance associated with the length of the current-carrying path bypassing the pores.

In recent decades, the electromagnetic properties and the possibility of application of disordered nanostructured carbon materials, such as glassy carbon have been actively studied because of their heat resistance, mechanical strength, and chemical stability. A promising way is the application of natural analogues of synthetic glassy carbon, primarily shungite.[14,15] Shungite is a carbonaceous rock, the carbon part of which is a natural analogue of low-temperature glassy carbon.[16–19] The complex structure of shungite provides effective absorption of radio emission in the frequency range from a few megahertz to tens and hundreds of terahertz.[20–22]

The applied properties of carbon materials are determined by their conductivity, which depends on the concentration of carbon in the material and its intrinsic conductivity.[22] The carbon content in shungite varies from 3 to 98% for samples from different deposits. Since the conductivity of shungite is controlled by disordered carbon, understanding its electrically conductive properties is extremely important.

Shungite carbon has a complex quasi-dispersed structure from stacks of graphene layers, which are sometimes grouped into globules and ribbons.[18,19,23,24] The sizes of the stacks are in units of nanometers, and the globule and ribbon sizes reach several tens of nanometers. However, the relative content of globules and ribbons in the shungite structure is small compared to the members. Chaotic distribution and orientation of graphene stacks[18,24] complicate the quantitative analysis of both their geometric parameters and the integral conductivity of shungite carbon.

The quasi-dispersion of the shungite structure leads to the formation of extended electrically conductive paths, often interrupted by structural defects. For shungite to be conductive at constant current (static conductivity), such paths must be closed. Microwave conductivity (dynamic) requires the circulation of currents inside the paths, without the required condition of their mutual overlap. An example of such structures is amorphous nanogranular composite films,[25] consisting of a conducting ferromagnetic metal in a dielectric matrix. They have high static and microwave conductivity,[26] the latter being provided by the mechanism of intragranular currents.[22] For shungites, a similar model of their microstructure was used by Golubev et al.[22] This model describes well the electrical properties of shungite

CONTACT Yevgeny Golubev yevgenygolubev74@mail.ru Institute of Geology of Komi SC, Russian Academy of Sciences, Syktyvkar, 167982, Russia
© 2023 Taylor & Francis Group, LLC

samples with a carbon content of <64%. For shungites with a carbon content of more than 75%, it is necessary to consider models of the conductivity of pure carbon taking into account the structural features of disordered carbon.

To analyze the conductivity of such structures, the method of current tubes was proposed by Antonets et al.,[27] where the current in a block limited in space flows through straight tubes without branching or passing from one tube to another. The tubes consist of a sequence of graphene stacks that follow one another at regular intervals.

The orientational disorder of stacks in shungite limits the capacity of the tube model. At the same time, it can be assumed that the statistical properties of the stacks are not very varied to prevent the use of the tube model. We propose an algorithm that makes it possible to reduce the chaotic nature of the structure of shungite carbon to a regular model that allows to use the tube model as a first approximation to the representation of an electroconductive model of disordered carbon using the example of shungite. Эта модель основана на геометрическом рассмотрении структуры, состоящей из элементов, проводимость которых задана, и не рассматривает механизмы транспорта электронов на электронно-атомном уровне.

This work is devoted to the theoretical analysis of the integral conductivity of disordered carbon based on the tube model for the example of shungite samples using the experimentally calculated structural parameters of these samples, as well as to the assessment of the effect on the conductivity of the sizes of graphene layers stacks and the gaps between them.

2. Objects and methods

To analyze the conductive properties of shungite carbon, typical samples of Karelian shungite with a carbon content of (97 ± 1)% from the Maxovo deposit (with integral conductivity (2500 ± 200) S/m) and Nigozero deposit (with conductivity (1500 ± 150) S/m) were selected[16,22]). The supermolecular structure of these samples was previously studied using STEM and described in Antonets et al.[28]

3. Results

3.1. The current tube model

In the model of current tubes, it is assumed that the current within a block limited in space flows through the tubes, without branching or passing from one tube to another. The block is a rectangular parallelepiped. Straight tubes are parallel to each other from one surface of the block to another and have a constant cross-section. They consist of graphene stacks following each other (Figure 1). This is an initial approximation to the model of non-crystalline carbon material. A typical carbon structure of shungites is shown in the inset in Figure 1. It can be seen from the figure that the stacks containing several parallel graphene layers are separated by gaps where the orientation of the layers is chaotic. The average sizes of stacks of graphene layers for Maxovo and Nigozero are (1.50 ± 1.12) and (2.39 ± 1.62) nm, respectively.[28]

The thickness of one graphene layer can be estimated from the covalent radius of the carbon atom as about 0.08 nm. In this case, taking into account the average interplanar distance in graphene stacks (0.3458 nm),[19] we obtain the size of the gap between the layers of 0.2658 nm. All of the above parameters will be further used to calculate the tube model.

For geometric parameters, we will use the following designations: *G*—graphene layer; *P*—stack; *T*—a tube; *B*—the gap between two graphene layers inside one stack; *D*—the gap between two adjacent stacks inside the tube; *H*—the gap between the two tubes inside the block; *S*—the block as a whole. For electrical parameters, we will use the designations: ρ—resistivity, σ—specific conductivity, *R*—absolute electrical resistance.

We will consider the tube structure within the framework of the model of regular distribution of stacks (scheme in Figure 1). Let us assume that all tubes are oriented along the same axis in the plane of the sample, and the graphene layers inside the stacks are parallel to the plane of the sample. The coordinate system is oriented in such a way that the plane Oxy is parallel to the planes of the graphene

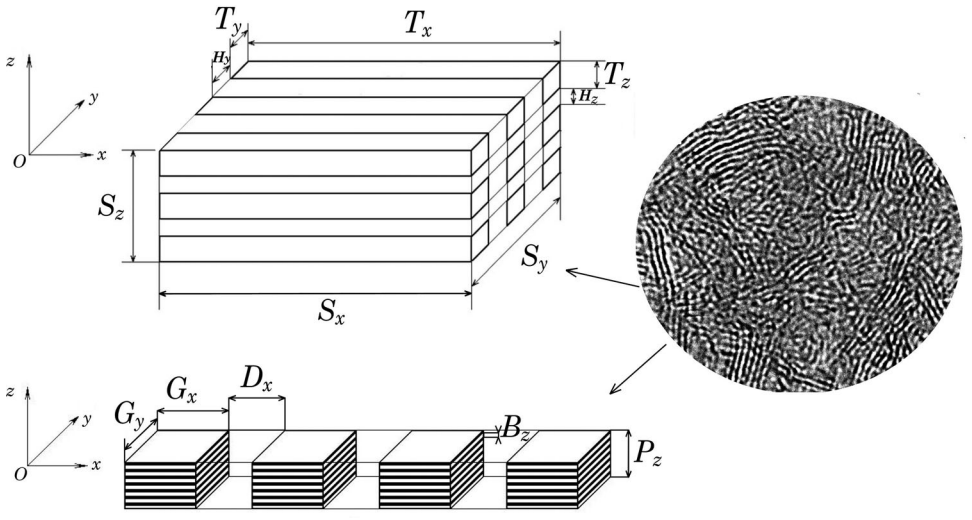

Figure 1. Schematic representation of the tube model. A block of parallel flow tubes (top) and a tube that consists of sequentially and evenly spaced packs of graphene layers (bottom). On the right is the structure of shungite carbon (fragment of STEM image).

layers, and the axis Oz is perpendicular to them. The current flows along the graphene layers.

3.2. Methods for calculating conductivity by the tube model

For calculations, we introduce the following geometric parameters:

S_x, S_y, S_z are block sizes along all coordinate axes;
G_x, G_y, G_z are the sizes of the graphene layer along all coordinate axes;
P_z is the size of the stack along the axis Oz;
B_z is the size of the gap between graphene layers inside the stack along the axis Oz;
D_x is the size of the gap between the stacks inside the tube along the axis Ox;
H_y and H_z are the sizes of the gaps between the tubes inside the block along the axes Oy and Oz.
We also define the following electrical parameters:
R_{Tx} is the absolute electrical resistance of the tube along the axis Ox;
R_{Gx} is the absolute electrical resistance of the graphene layer along the axis Ox;
R_{Px} is the absolute electrical resistance of the stack along the axis Ox;
R_{Bx} is the absolute electrical resistance of the gap between graphene layers along the axis Ox;
R_{Dx} is the absolute electrical resistance of the gap between the stacks along the axis Ox;
ρ_{Gx} is the resistivity of the graphene layer along the axis Ox;
ρ_{Bx} is the resistivity of the gap between graphene layers inside the stack along the axis D_x;
ρ_{Dx} is the resistivity of the gap between stacks in the tube along the axis Ox;
ρ_{Hx} is the resistivity of the gap between the tubes inside the block along the axis Ox.

Let's first consider one layer of graphene. If its dimensions in three coordinates G_x, G_y, G_z, as well as the resistivity ρ_{Gx} along the axis Ox are specified, then the electrical resistance of the graphene layer:

$$R_{Gx} = \frac{\rho_{Gx} G_x}{G_y G_z} \tag{1}$$

We believe that the stack consists of graphene layers of the same size, lying exactly one above the other, therefore, the dimensions of the gap between two graphene layers along the axes Ox and Oy are equal G_x and G_y, respectively, and along the axis Oz is equal B_z. Then, the electrical resistance of the gap between graphene layers along the axis Ox will take the form:

$$R_{Bx} = \frac{\rho_{Bx} G_x}{G_y B_z} \tag{2}$$

Let us assume that the stack contains N_{Pz} graphene layers. Since graphene layers alternate with gaps, it contains $N_{Pz} - 1$ gaps. Thus, the size of the stack along the axis Oz is:

$$P_z = N_{Pz} G_z + (N_{Pz} - 1) B_z \tag{3}$$

From relation (3), we find the number of graphene layers in a stack:

$$N_{Pz} = \frac{P_z + B_z}{G_z + B_z} \tag{4}$$

Now let's find the electrical resistance of the stack R_{Px} along the axis Ox. This resistance is formed by the parallel connection of the resistances of the graphene layers and gaps along this axis. The resistance of the parallel-connected layers N_{Pz} is R_{Gx}/N_{Pz}, and the resistance of the parallel-connected gaps is $R_{Bx}/(N_{Pz} - 1)$. Since these resistances in the stack are also connected in parallel, the stack resistance along the axis Ox will take the form:

$$R_{Px} = \left(\frac{N_{Pz}}{R_{Gx}} + \frac{N_{Pz} - 1}{R_{Bx}} \right)^{-1} = \frac{R_{Gx} R_{Bx}}{N_{Pz} R_{Bx} + (N_{Pz} - 1) R_{Gx}} \tag{5}$$

After calculating the electrical parameters for one stack, we proceed to calculate the electrical parameters of the tube. If the block dimensions S_x, S_y, S_z, are specified, then the tube length along the axis Ox is equal to the block length S_x, and the dimensions along the other two axes are determined by the size of the stack along these axes, that is, along the axis Oy by the size of the graphene layer G_y, and along the axis Oz by the size of the stack P_z. The space between stacks inside the tube is sized D_x. The dimensions of the gap along the other two axes are determined by the dimensions of the stack G_y and P_z, respectively.

Let the tube contain N_{Tx} stacks and $N_{Tx} - 1$ gaps. Then the total tube length, equal to the block length S_x is:

$$S_x = N_{Tx} P_x + (N_{Tx} - 1) D_x \tag{6}$$

From equation (6), the number of stacks in the tube is expressed as:

$$N_{Tx} = \frac{S_x + D_x}{G_x + D_x} \tag{7}$$

The current flows only along the tube; therefore, we will further evaluate the tube resistance along the axis Ox. This resistance is the sum of the resistances of stacks R_{Px} and gaps R_{Dx}. If the specific resistance of the gap ρ_{Dx} along the axis Ox is specified, then the electrical resistance of the gap can be defined as:

$$R_{Dx} = \frac{\rho_{Dx} D_x}{G_y P_z} \tag{8}$$

The total resistance of the tube along the axis Ox is the resistance of the series-connected resistances of the stacks N_{Tx} and the resistances of the gaps $N_{Tx} - 1$:

$$R_{Tx} = N_{Tx} R_{Px} + (N_{Tx} - 1) R_{Dx} \tag{9}$$

Now let's move on to calculating the resistance along the axis Ox for the block as a whole. Along the axes Oy and Oz the tubes are spaced at equal intervals H_y and H_z,

respectively. If these gaps are given, then the total block size along these axes:

$$S_y = N_{Sy}G_y + (N_{Sy} - 1)H_y; \quad (10)$$

$$S_z = N_{Sz}P_z + (N_{Sz} - 1)H_z, \quad (11)$$

where the number of tubes, placed in the block N_{Sy} and N_{Sz}:

$$N_{Sy} = \frac{S_y + H_y}{G_y + H_y}; \quad (12)$$

$$N_{Sz} = \frac{S_z + H_z}{P_z + H_z}. \quad (13)$$

The number of tubes over the cross-section of the block is $N_{Sy}N_{Sz}$. The area occupied by all tubes in the cross-section of the block is $N_{Sy}N_{Sz}G_yP_z$, and the area of the entire block in the cross-section is S_yS_z. Subtracting the transverse area of all tubes from the transverse area of the block, we obtain the total transverse area of the gaps $S_yS_z - N_{Sy}N_{Sz}G_yP_z$.

The total resistance of all tubes connected in parallel across the cross-section of the block is $R_{Tx}/(N_{Sy}N_{Sz})$. If the specific resistance of the gaps ρ_{Hx} along the axis Ox is specified, then the total resistance of all gaps is determined by the expression $\rho_{Hx}S_x/(S_yS_z - N_{Sy}N_{Sz}G_yP_z)$, taking into account that the length of each of the gaps is equal to the length of the block S_x. The total resistance of the block is determined by the parallel connection of the resistances of all tubes and the resistance of all gaps:

$$R_{Sx} = \left(\frac{N_{Sy}N_{Sz}}{R_{Tx}} + \frac{S_yS_z - N_{Sy}N_{Sz}G_yP_z}{\rho_{Hx}S_x}\right)^{-1} \quad (14)$$

or after mathematical transformations:

$$R_{Sx} = \frac{\rho_{Hx}S_xR_{Tx}}{\rho_{Hx}S_xN_{Sy}N_{Sz} + R_{Tx}(S_yS_z - N_{Sy}N_{Sz}G_yP_z)} \quad (15)$$

Block resistivity along the axis Ox is:

$$\rho_{Sx} = \frac{R_{Sx}S_yS_z}{S_x} \quad (16)$$

If we substitute (15) in (16) we get:

$$\rho_{Sx} = \frac{\rho_{Hx}S_yS_zR_{Tx}}{\rho_{Hx}S_xN_{Sy}N_{Sz} + R_{Tx}(S_yS_z - N_{Sy}N_{Sz}G_yP_z)} \quad (17)$$

Finally, the specific conductivity of the block as a whole along the axis Ox is the reciprocal of (17), that is:

$$\sigma_{Sx} = \frac{\rho_{Hx}S_xN_{Sy}N_{Sz} + R_{Tx}(S_yS_z - N_{Sy}N_{Sz}G_yP_z)}{\rho_{Hx}S_yS_zR_{Tx}} \quad (18)$$

In this formula, the parameters S_x, S_y, S_z can be chosen arbitrarily, and if they are 10^3 nm and more, then according to Antonets et al.,[27] the resistivity does not depend on them.

3.3. Theoretical calculations within the tube model

For calculations, geometric parameters G_x, G_y, G_z, P_z, B_z, D_x, H_y, H_z were previously estimated for samples of shungite from the Maxovo and Nigozero deposits based on the analysis of STEM images.[28] The resistivity of graphene along its plane $\rho_{Gx} = 2.5 \cdot 10^{-8}\Omega \cdot m$ is known from the literature.[29,30]

We estimate the resistivity of the gap between graphene layers inside the stack by four orders of magnitude higher: $\rho_{Bx} = 10^{-4}\Omega \cdot m$–$10^{-3}\Omega \cdot m$. Considering that the indicated resistance was determined for graphite with an interplanar distance between graphene layers of 0.335 nm, and in shungites this distance was increased to 0.347–0.350 nm, the real resistance between the layers can be even higher. However, in this work, we will take the value of graphite resistance as a basis. We will consider the parameter ρ_{Dx} to be comparable to ρ_{Bx}:

$$\rho_{Dx} = N_{Dx}\rho_{Bx} \quad (19)$$

where N_{Dx} is a numerical coefficient, from several tenths to several units. In further calculations for simplicity $N_{Dx} = 1$.

Taking into account that the integral conductivity of the structure is determined by the tubes, the value of the resistivity of the gaps between the tubes should be taken at least 5–10 times more than ρ_{Dx}. When calculating, we will assume $\rho_{Hx} = 2.5 \cdot 10^{-3}\Omega \cdot m$. Verification shows that with all other parameters unchanged, an increase ρ_{Hx} above this value does not affect the value of the integral conductivity. The key geometrical parameters controlling the conductivity in the proposed model are the sizes of stacks of graphene layers and the size of the gaps between them. For samples from the Maxovo and Nigozero deposits in Antonets et al.,[28] the average sizes of the stacks and the size distributions having a lognormal appearance were determined. For the sizes of the intervals between the stacks, we know only the average sizes. Further, within the framework of the tube model, the following calculations were carried out: determination of the dependence of the integral conductivity on the average size of the stack; assessment of the contribution of the lognormality of the size distribution of stacks to the integral conductivity; assessment of the specific and electrical resistance of tubes depending on the size of the gaps between the stacks of graphene layers; determination of the resistance of the gaps between the stacks.

3.4. Parameter values used in the current tube model

We used the following values in the calculations of the current tube model:

Geometric parameters:

$$S_x = 3000\,nm, S_y = 1000\,nm, S_z = 1000\,nm; G_z = 0.08\,nm; B_z = 0.2658\,nm;$$

Electrical parameters:

$$\rho_{Gx} = 2.5 \cdot 10^{-8}\Omega \cdot m; \rho_{Hx} = 2.5 \cdot 10^{-3}\Omega \cdot m;$$
$$\rho_{Bx} = 0.5 \cdot 10^{-3}\Omega \cdot m.$$

The values of the remaining parameters varied for each test sample (Table 1). The integral conductivity of the samples was obtained using the four-probe method.[22]

Table 1. Geometric parameters based on the results in Antonets et al.[28]

	$\sigma_x, S/m$	G_x, nm	G_y, nm	P_z, nm	H_y, nm	H_z, nm	D_x, nm
Maxovo	2500	1.50	1.50	1.50	1.11	1.11	1.11
Nigozero	1500	2.39	2.39	2.39	2.11	2.11	2.11

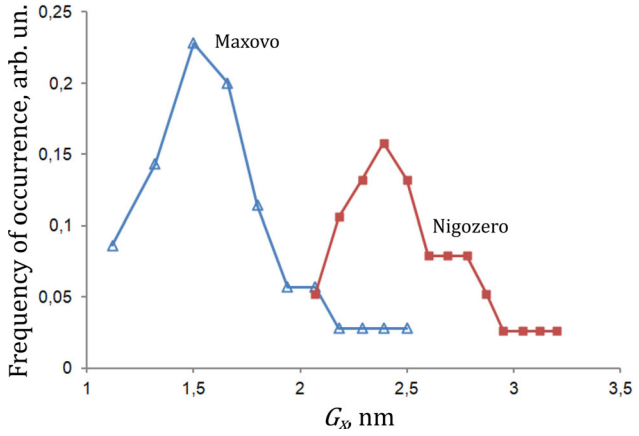

Figure 2. The size distributions of packs were obtained for the Maxovo and Nigozero samples.[25]

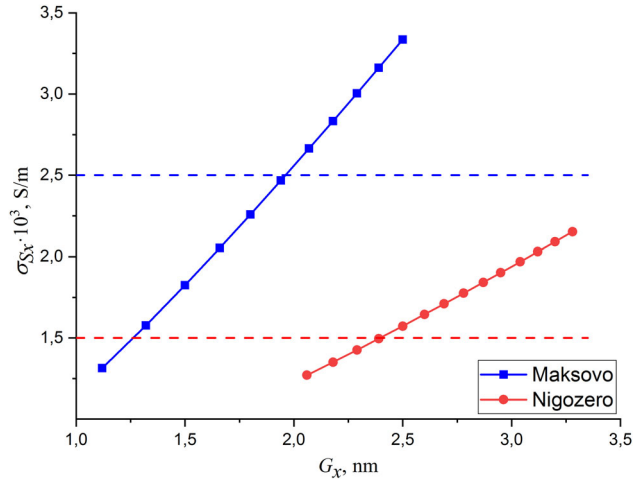

Figure 3. The specific conductivity σ_{Sx} *vs.* the stacks size *Gx*.

3.5. Dependence of the specific conductivity on the size of stacks and the distribution of their sizes

Lognormal size distributions of stacks for the Maxovo and Nigozero samples were obtained in the work.[28] These distributions (Figure 2) were taken as the basis for calculating the dependence of the specific conductivity σ_{Sx} on the stacks size G_x using the formula (18) (Figure 3). The sizes of stacks G_y and P_z change similarly G_x.

As seen in Figure 3, with an increase in the size of the stacks, the conductivity of the samples increases, this corresponds to the classical concepts. In this case, the conductivity of the Maxovo sample grows faster than the conductivity of the Nigozero sample and has large values for the same stacks sizes. For example, the Maxovo sample conductivity is more than twice that of Nigozero sample when $G_x = 2.5nm$.

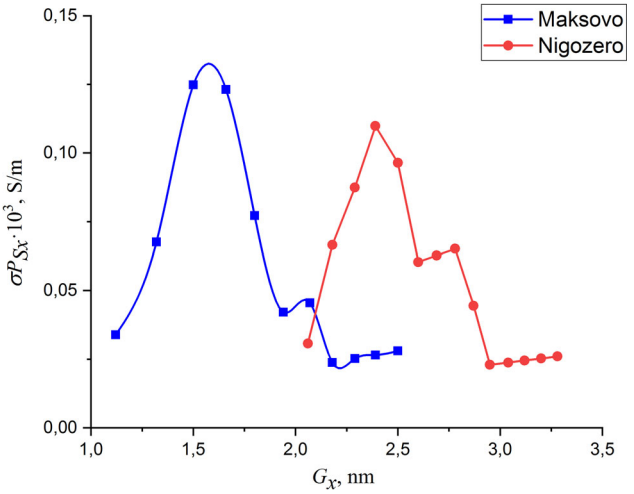

Figure 4. The specific conductivity taking into account frequency of occurrence σP_{Sx} as function the stacks size *Gx*.

Let us consider the dependence of the specific conductivity on the size of the stacks G_x taking into account their frequency of occurrence σP_{Sx}. For this, we normalize to the maximum value of specific conductivity σ_{Sx} (Figure 3) for the Maxovo $(3.335 \cdot 10^3 S/m)$ and Nigozero $(2.153 \cdot 10^3 S/m)$ samples, and then multiply the resulting value by P_x. As seen from Figure 4, the key contribution to the conductivity of the samples is made by stacks in the size range 1.4–1.75 nm for Maxovo and 2.20–2.80 nm for Nigozero, which is determined by the shape of the size distribution of the stacks. The modal size of the stacks at the maximum conductivity is 1.6 nm for Maxovo and 2.4 nm for Nigozero.

Let us compare this result with the calculations of the tube model. The maximum conductivity for the Maxovo and Nigozero samples is the integral conductivity of the whole sample, shown in Table 1.

The straight line of integral conductivity intersects the dependence for Nigozero (Figure 3) at a point $G_x = 2.4nm$, which exactly coincides with the experimentally estimated modal size of stacks (Figure 4), and for Maxovo, the intersection occurs at a point $G_x = 1.9nm$, which differs from the stacks size obtained experimentally (1.6 nm). This difference is probably due to the fact that we consider the resistivity of the gap between the tubes inside the block $\rho_{Hx} = 2.5 \cdot 10^{-3}\Omega \cdot m$ to be the same for Maxovo and Nigozero. The condition for the correspondence of the modal size of the stacks with the maximum conductivity to their experimental value (1.6 nm) is the resistivity of the gap between the tubes in the Maxovo sample $\rho_{Hx} = 0.8 \cdot 10^{-3}\Omega \cdot m$.

3.6. Dependence of conductivity on the gap size between the stacks in the tube

The average gap size between the stacks for Maxovo and Nigozero was calculated by Antonets et al.[28] To estimate the dependence of the conductivity σ_{Sx} on the size of the gaps between the stacks in the tube D_x, we plotted these dependences in a specially selected range of gap sizes (0.6–1.6 nm for Maxovo and 1.4–2.7 nm for Nigozero with an

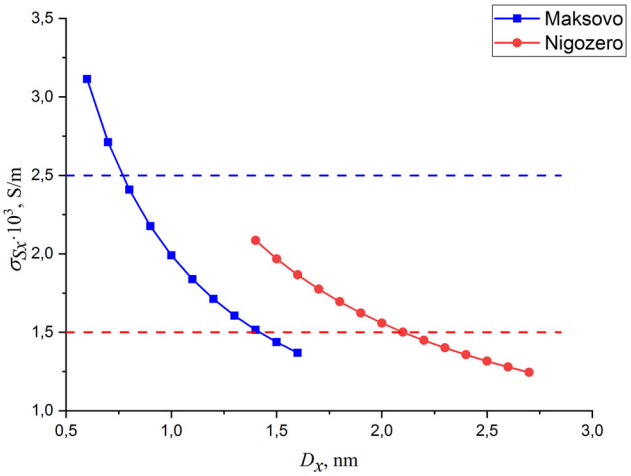

Figure 5. The specific conductivity σ_{Sx} *vs.* the gaps size *Dx*.

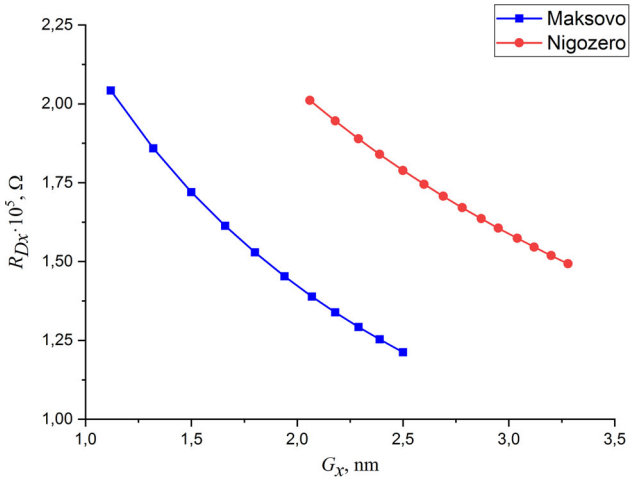

Figure 6. The absolute electrical resistance of the gap R_{Dx} *vs.* the stacks size G_x for the Maxovo (squares) and Nigozero (circles) samples.

interval of 0.1 nm) using expression (18). The calculations assume that the size of the gaps between the tubes H_y changes in the same way as D_x. The values of the remaining parameters were used according to Table 1.

The specific conductivity σ_{Sx} decreases with an increase in the gaps size D_x (Figure 5), which corresponds to the classical concepts. The conductivity of the Maxovo sample decreases faster with increasing D_x than the conductivity of Nigozero sample. Dotted straight lines in Figure 5 correspond to the integral conductivity of the sample. The intersection of the dashed straight line with the curve for the Nigozero sample occurs at a point $D_x = 2.1nm$, and for the Maxovo sample at a point $D_x = 0.8nm$. Here again, it is interesting that for Nigozero the experimental[28] and calculated results coincide, while for Maxovo the calculated size of the gaps (0.8 nm) is much smaller than the experimental one (1.1 nm). To coincide with the experimental result, it is necessary to reduce the value of the resistance between the tubes for the Maxovo sample in the calculations.

3.7. Specific resistance of the gap between stacks in a tube

One of the key tasks is to determine the specific and absolute electrical resistance of the gap between the stacks in the tube. To quantitative estimate the electrical resistance of the gap R_{Dx}, we use equation (9), according to which:

$$R_{Dx} = \frac{R_{Tx} - N_{Tx}R_{Px}}{N_{Tx} - 1} \tag{20}$$

In relation (20), we do not know the electrical resistance of the tube R_{Tx}, and the remaining parameters can be determined from equations (5) and (7). We express the unknown resistance of the tube from relation (18), taking as σ_{Sx} the integral conductivity of the samples from Table 1:

$$R_{Tx} = \frac{\rho_{Hx}S_xN_{Sy}N_{Sz}}{\sigma_{Sx}\rho_{Hx}S_yS_z - S_yS_z + N_{Sy}N_{Sz}G_yP_z} \tag{21}$$

By calculating the tube resistance R_{Tx} and substituting its value into equation (20), it is possible to determine the electrical resistance of the gap between the stacks in the tube R_{Dx}, and estimate the specific resistance of the gap ρ_{Dx} from relation (8):

$$\rho_{Dx} = \frac{R_{Dx}G_yP_z}{D_x} \tag{22}$$

According to (20) and (22), the electrical and specific resistivity of the gap between the stacks in the tube depends on the resistance of the stack R_{Px} (equation 5), which is determined by the resistance of the graphene layer R_{Gx} and the resistance of the gap between the graphene layers R_{Bx} (equations 1 and 2, respectively). The resistance R_{Gx} (hundreds of ohms) is 3–4 orders of magnitude less than the resistance R_{Bx} (units of $M\Omega$), therefore $R_{Gx} \ll R_{Bx}$, and in expression (5) the term including the resistance of the graphene layer in the denominator can be neglected.

This will greatly simplify the calculation of the stack resistance:

$$R_{Px} = \frac{R_{Gx}}{N_{Pz}} \tag{23}$$

This simplification makes it possible to completely exclude from consideration the parameter R_{Bx} and, therefore ρ_{Bx}.

3.8. Dependence of absolute electric resistance of the gap between stacks on stack size

Figure 6 shows the dependences of the absolute electrical resistance of the gap between the stacks R_{Dx}, calculated by formula (20), on the size of the stacks G_x for the Maxovo (squares) and Nigozero (circles) samples. The absolute electrical resistance R_{Dx} is primarily determined by the contact area of the stacks of graphene layers. Figure 6 reveals that the qualitative form of the dependences for the Maxovo and Nigozero samples is practically the same. With a change in the contact area of the stacks of graphene layers, the electrical resistance of the graphene layer of the samples R_{Gx} (equation 1) is retained (312.5 for the Maxovo and Nigozero samples). Due to the fact that the number of graphene layers in a stack increases due to an increase in the stack size

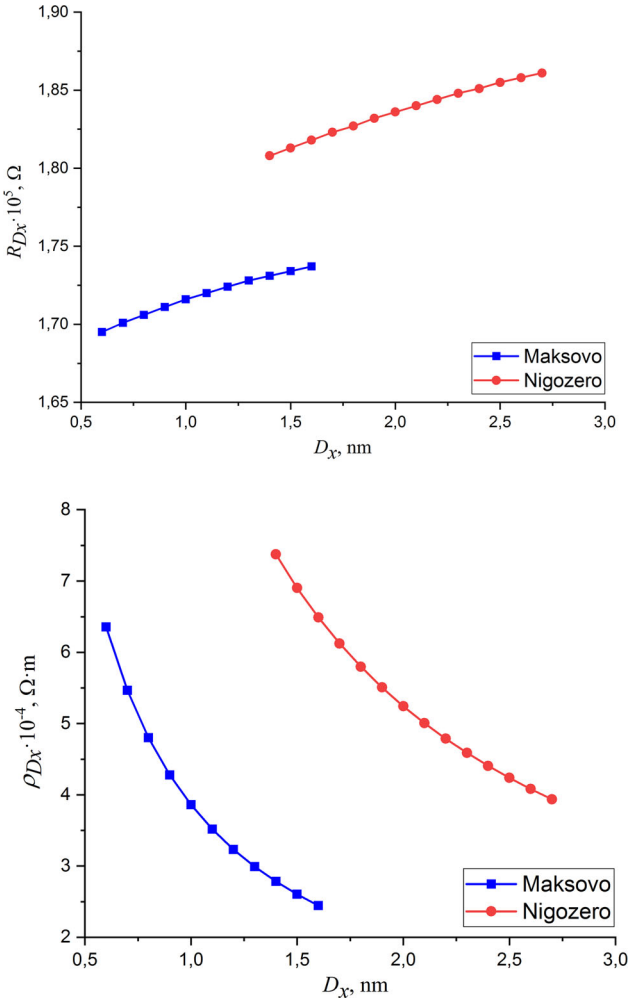

Figure 7. Dependences R_{Dx} (a) and ρ_{Dx} (b) on the gap size D_x for the Maxovo (squares) and Nigozero (circles) samples.

(formula 4), the electrical resistance of the stacks R_{Px} decreases (formula 23), while the number of stacks in the tube also decreases. Thus, the electrical resistance of the stack R_{Px} falls significantly less than the tube electrical resistance R_{Tx}. Therefore, the electrical resistance of the gap between the stacks also decreases as the stacks size increases.

3.9. Dependence of absolute electric resistance and specific resistance of the gap between stacks on the gap size

The dependences of the absolute electrical resistance R_{Dx} and specific resistivity ρ_{Dx} of the gap between the stacks on the size of this gap D_x for the Maxovo and Nigozero samples were calculated using equations (20) and (22), respectively. The electrical resistance of the gap increases with an increase in its size insignificantly (within the limits $0.042\cdot10^5\Omega$ for Maxovo and $0.053\cdot10^5\Omega$ for Nigozero) and nonlinearly. The size of the gap affects the tube electrical resistance R_{Tx} and the number of stacks in the tube, and the contribution to both of these parameters is almost the same, which leads to an insignificant change in the electrical resistance of the gap R_{Dx} (Figure 7a). Due to this, the specific resistivity of the gap ρ_{Dx} at a weakly changing electrical

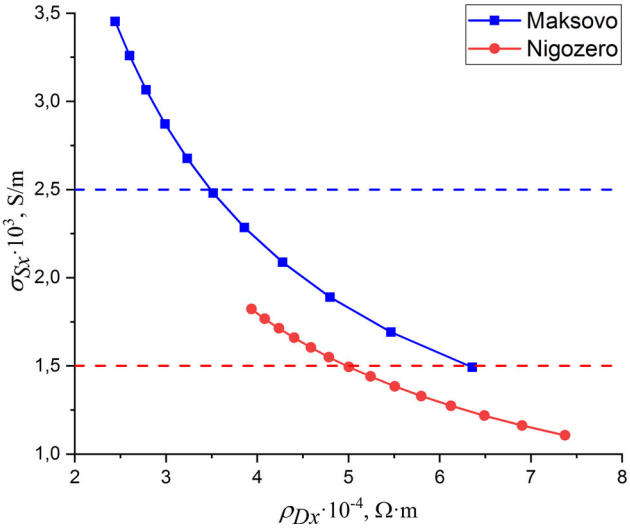

Figure 8. The dependences of the conductivity σ_{Sx}, calculated by equation (18), on the resistivity of the gap between the stacks ρ_{Dx} for the Maxovo (squares) and Nigozero (circles) samples. The dotted lines mark the integral conductivity of the whole sample for the Maxovo and Nigozero samples, shown in Table 1.

resistance of the gap and constant dimensions of the stacks G_y and P_z depends on the size of the gap (equation 22) as inverse proportionality (Figure 7b).

3.10. Quantitative estimation of the specific resistance of gap between stacks and the size of the gap

Dependencies in Figures 7 and 8 show the ratios of conductivity, electrical and specific resistivity of gaps, and the sizes of these gaps. So, if the integral conductivity σ_x is known (Table 1), then by marking this point on the vertical axis and drawing a horizontal line through it until it intersects with the curve, you can get a one-to-one correspondence between ρ_{Dx}, R_{Dx}, and D_x. A similar correspondence can be obtained for the stacks.

Figure 8 shows that the dashed lines corresponding to the experimental conductivity of 2500 S/m for the Maxovo sample and 1500 S/m for the Nigozero sample intersect the curves at the resistivity $3.55\cdot10^{-4}\Omega\cdot m$ and $5.00\cdot10^{-4}\Omega\cdot m$, respectively. Figure 7b shows that these resistivities correspond to gap values of 1.1 nm for the Maxovo sample and 2.1 nm for the Nigozero sample. It is these values of the gaps that were obtained experimentally.[28] However, if we compare the values of the gaps with those obtained from Figure 5, it can be seen that for the Maxovo samples, they diverge (1.1 nm and 0.8 nm), while for the Nigozero samples, they coincide (2.1 nm). We suggest the following reason for this discrepancy. For Figures 7 and 8, we used the gaps between the stacks in the range of 0.6–1.6 nm for the Maxovo sample and 1.4–2.7 nm for the Nigozero sample. For these values of the gaps, the resistivity was calculated (Figure 6b), and, accordingly, the specific conductivity was determined (Figure 8). In Figure 5, when calculating the specific conductivity of the stacks, the resistivity of the gaps was determined according to the relation (19), in which $\rho_{Bx}=0.5\cdot10^{-3}\Omega\cdot m$ (section "Values of the parameters

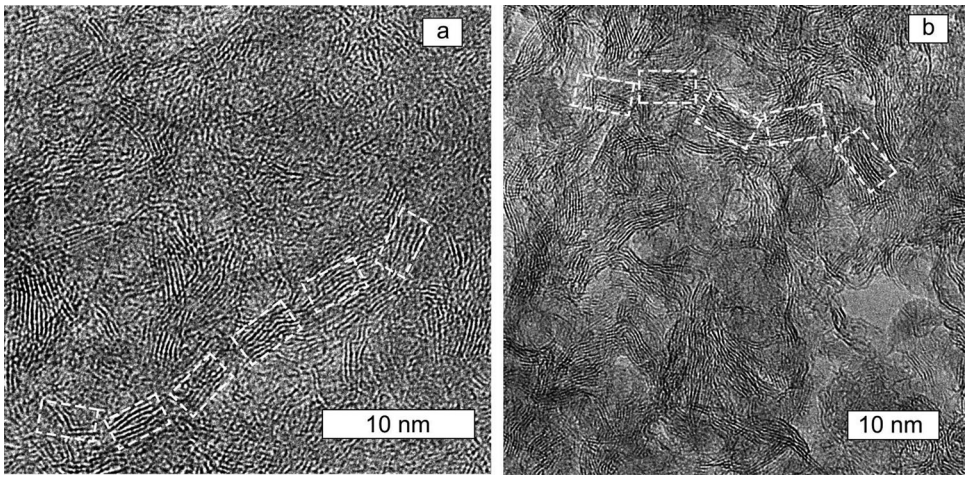

Figure 9. STEM images of samples Maxovo (a) and Nigozero (b). The dotted squares highlight the possible paths for the current to flow through the stacks of graphene layers within the current tubes.

used in the model of current tubes"), and the proportionality coefficient was $N_{Dx} = 1$. As a result, the resistivity of the gaps for the Maxovo and Nigozero samples in the current tube model is identical $5.00 \cdot 10^{-4}\Omega \cdot m$. Since for the Nigozero sample the resistivity in Figures 5, 7b, and 8 coincide, then the intervals between stacks for both methods are the same. For Maxovo samples, the resistivity of the gaps between the stacks is different ($3.55 \cdot 10^{-4}\Omega \cdot m$ according to Figures 7b and 8 and $5.00 \cdot 10^{-4}\Omega \cdot m$ according to Figure 5), which leads to different sizes. To obtain the desired value of the gap $D_x = 1.1nm$ for a given specific conductivity of 2500 S/m using the model of current tubes (in Figure 5), at a fixed value $\rho_{Bx} = 0.5 \cdot 10^{-3}\Omega \cdot m$ in relation (19), it is necessary to take the proportionality coefficient numerically equal to the ratio $3.55 \cdot 10^{-4}/5.00 \cdot 10^{-4}$, i.e. $N_{Dx} = 0.71$.

4. Discussion

This work is devoted to a promising approach for quantifying the effect of structural factors on electrical conductivity in disordered nanostructured carbon materials within the framework of the current tube model. It is very difficult to identify structural regularities in disordered materials; therefore, at this stage, the model was simplified by describing stacks of graphene layers that are complex in shape and chaotic in contacts in the form of regular and parallel tubes. The actual distribution structure of graphene stacks is quite complex, as shown by STEM images (Figure 9). The current in such a structure does not flow along straight lines but along winding trajectories determined by the local configuration of the stacks. The calculation of current flow paths here is extremely complicated. But, due to the absence of a single selected direction, it can be assumed that the current is distributed more or less evenly over the entire area. We propose an approximate model of a uniform distribution in the form of a set of parallel tubes, within which the current flows in straight lines. This means that the tubes must be considered isolated from each other. The reduction of calculations is achieved precisely by the transition from a uniform, but random distribution to the same uniform, but geometrically ordered, allowing the calculation we proposed. In addition, for graphite, the conductivity along the graphene layer and across the layers differ by a factor of 10,000. Accordingly, it is always more advantageous for the current to flow along the layers in the stack. Despite the rather rough initial approximation, in mathematical terms, such an approximation made it possible to obtain a completely correct quantitative assessment of the influence of structural factors on the conductivity and to present quite achievable prospects for assessing this influence with a closer to the real structure.

Interestingly, when comparing the calculated results with the experimentally measured structural and electrical parameters of the samples, we obtained different results. While for the Nigozero sample, we showed the coincidence of the calculated (Figures 4, 6, and 7) and experimentally measured[25] parameters, for the Maxovo sample we obtained different results for the dependences of conductivity and resistance on the size of the gaps between the stacks and the stacks size. This discrepancy can be explained in two ways. First, regions of contacts between stacks of graphene layers for the Nigozero and Maxovo samples can have different chemical and geometric structures. Therefore, the electrically conductive properties of contacts between stacks, even without taking into account their size, can differ sharply. Therefore, it is necessary to use different proportionality coefficients N_{Dx} in the equation (19). This can be confirmed by the sharply different ratios of the intensities of the I_{D2}/I_G bands of the Raman spectra of these samples,[31] since the D band in glassy carbon is associated with structural defects at the edges of graphene bands, such as breaks of graphene networks or inclusions of heteroelements at the edges of graphene layers.[19] The second explanation is related to the possible different correspondence of the sample structure to the tube model. In general, the used model of current tubes is more comparable to the band or band-stack models of the structure of glassy carbon and its natural analogs. If we analyze typical high-resolution STEM images of the structure of the Maxovo and Nigozero samples (Figure 9), it can be seen that the curved-band model of the structure is more

characteristic of the Nigozero sample than of the Maxovo sample. In the Maxovo sample, there are many regions of an almost continuous close-packed stacks nanostructure. Additionally, the packing density in Maxovo shungite is higher than that from Nigozero, which is confirmed by the results of the statistical analysis of STEM images (the gaps size in Maxovo is two times smaller than in Nigozero). The tube model assumes that current flows only within the tube and does not transfer from one tube to another. Due to the high bulk density of the arrangement of graphene stacks in Maxovo, it is difficult to distinguish isolated "tubes" in its structure. It is most likely that in the Maxovo sample the current passes between the "tubes," which is confirmed in our model by the coincidence of the calculated parameters with the experimental ones when the resistance between the tubes decreases to the value of the resistance between the stacks inside the tube. This, in turn, shows that the tube model does not fully reflect the structure of Maxovo shungite and makes it possible to find the limits of applicability of the tube model for synthetic and natural disordered carbon materials. Such approach facilitates to better understand the complex structure of disordered carbon materials.

The above calculations make it possible to determine only the relationship between the resistances ρ_{Bx} and ρ_{Dx}, given by the parameter N_{Dx}. However, if one of these parameters can be found from independent experiment or model calculation, then it will be possible to estimate the absolute values of the electrical parameters of the stacks and gaps.

In origin samples, the stacks are oriented in a rather arbitrary manner, which should lead to a completely isotropic character of the conductivity of the sample as a whole. That is, the parameters of the structure should be averaged taking into account the arbitrary orientation of the stacks. For such averaging, one can use the methodical approach described in detail by Shavrov and Shcheglov,[32] designed to determine the frequency of ferromagnetic resonance in a medium of anisotropic ferrite spheres. The authors leave this averaging procedure as applied to the tube model as a task for the following study.

5. Conclusion

In this work, a theoretical analysis of the effect of nanostructure parameters on the conductivity of disordered sp^2 carbon was carried out using the structural approximation in the form of a current tube model. The chaotic nature of the structure of shungite carbon was reduced to a regular model of parallel conductive tubes consisting of sequentially located stacks of graphene layers, as a first approximation to the representation of an electrically conductive model of shungite. The comparison of the model with the real structure was made using the example of two samples of natural disordered shungite carbon from different deposits (Maxovo and Nigozero), the structure of which is similar to synthetic glassy carbon, but has some differences relative to each other.

The dependences of the specific conductivity on the experimentally estimated sizes of stacks, taking into account the frequency of occurrence, and on the size of the gaps between the stacks, are investigated. The model was used to determine the modal size of the stacks and the gaps between the stacks, corresponding to the maximum specific conductivity of the samples for the combination of these parameters: 1.6 and 1.1 nm for Maxovo and 2.4 and 2.1 nm for Nigozero, respectively. It is shown that if for both samples the resistivity of the gaps between the stacks in the tube and between the graphene layers inside the stack is taken to be the same, then to obtain the above dimensions of the stacks and gaps for the Maxovo samples, it is necessary to reduce the resistivity between the tubes by almost three times from $2.5 \cdot 10^{-3}\Omega \cdot m$ to $0.8 \cdot 10^{-3}\Omega \cdot m$. However, in this case, the current can no longer flow along the tubes only, but also between them, which contradicts the very concept of the tube model. Therefore, for the same values of the resistivity of the gaps between the stacks in the tube and between the graphene layers inside the stack, the tube model does not fully reflect the structure of Maxovo shungite and makes it possible to determine the limits of applicability of this model.

Additionally, the work investigated the dependence of the absolute electrical resistance and specific resistivity of the gap between the stacks on the size of the stacks and the gap between the stacks. It was shown that the electrical resistance of the gap between the stacks significantly decreases with an increase in the size of the stacks (by 1.69 times for the Maxovo samples and by 1.35 times for the Nigozero samples), but at the same time, it weakly responds to an increase in the size of the gap between the stacks (increases within 3% for both samples), due to which the resistivity of the gap between the stacks depends on the size of the gap as inverse proportion. The relationship was established between the resistivity of the gaps between the stacks in the tube and between the graphene layers inside the stack. It is shown that for the Nigozero samples, both of these quantities are identical, and for the Maxovo samples, for a correct assessment of the electrical parameters, the proportionality coefficient must be taken into account. Under such conditions, the model of current tubes makes it possible to unambiguously establish a correspondence between resistivity, electrical resistance, and the size of gaps, as well as stacks. All electrical and dimensional characteristics estimated using the algorithm coincided with the experimental ones for the Maxovo and Nigozero samples.

Acknowledgements

The work was carried out within the framework of the state task of the Institute of Radio Engineering and Electronics named after V.A. Kotelnikov RAS (V.S.) and as part of research topics of the Institute of Geology of Komi SC of RAS (Ye.G.). We thank Alexandr S. Prikhodko and Nikolay I. Borgardt for studying the samples by the STEM.

Disclosure statement

No potential conflict of interest was reported by the author(s).

Data availability statement

Data will be made available on request.

References

[1] Beguin, F.; Frakowiak, E. *Carbons for Electrochemical Energy Storage and Conversional Systems*; CRS Press, **2010**.

[2] Pandolfo, A. G.; Hollenkamp, A. F. Carbon Properties and Their Role in Supercapacitors. *J. Pow. Sources* **2006**, *157*, 11–27. DOI: 10.1016/j.jpowsour.2006.02.065.

[3] Frackowiak, E.; Béguin, F. Carbon Materials for the Electrochemical Storage of Energy in Capacitors. *Carbon* **2001**, *39*, 937–950. DOI: 10.1016/S0008-6223(00)00183-4.

[4] Zhang, Y.; Feng, H.; Wu, X.; Wang, L.; Zhang, A.; Xia, T.; Dong, H.; Li, X.; Zhang, L. Progress of Electrochemical Capacitor Electrode Materials: A Review. *Hydrogen Energy* **2009**, *34*, 4889–4899. DOI: 10.1016/j.ijhydene.2009.04.005.

[5] Kazantseva, N. E.; Ryvkina, N. G.; Chmutin, I. A. Promising Materials for Microwave Absorbers. *J. Commun. Technol. Electron.* **2003**, *48*, 173–184.

[6] Chung, D. D. L. Electromagnetic Interference Shielding Effectiveness of Carbon Materials. *Carbon* **2001**, *39*, 279–285. DOI: 10.1016/S0008-6223(00)00184-6.

[7] Chung, D. D. L. Carbon Materials for Structural Self-Sensing, Electromagnetic Shielding and Thermal Interfacing. *Carbon* **2012**, *50*, 3342–3353. DOI: 10.1016/j.carbon.2012.01.031.

[8] Liang, J.; Wang, Y.; Huang, Y.; Ma, Y.; Liu, Z.; Cai, J.; Zhang, C.; Gao, H.; Chen, Y. Electromagnetic Interference Shielding of Graphene/Epoxy Composites. *Carbon* **2009**, *47*, 922–925. DOI: 10.1016/j.carbon.2008.12.038.

[9] Wang, Y.; Jiang, T.; Shi, S.; Xiang, L.; Tang, B.; Qi, Z.; Gui, X.; Cao, S.; Xu, K.; Li, W.; et al. Lightweight Chopped Carbon Fiber/Carbon Composites with Low Thermal Conductivity Fabricated by Vacuum Filtration Method. *Fuller. Nanotub. Carbon Nanostruct.* **2023**, *31*, 605–612. DOI: 10.1080/1536383X.2023.2194638.

[10] Moshnikov, I. A.; Kovalevski, V. V.; Markovskii, Y. A. Electrical Conductivity of Carbon Films Obtained by Thermal Sputtering of Type I Shungite Rocks of Various Deposits. Proceedings of 15th International Conference "Advanced Carbon Nanostructures" (ACNS'2021), **2022**; Vol. 30, pp 1–4. DOI: 10.1080/1536383X.2021.1998004.

[11] Kotsyubynsky, V.; Rachiy, B.; Boychuk, V.; Budzulyak, I.; Turovska, L.; Hodlevska, M. Correlation between Structural Properties and Electrical Conductivity of Porous Carbon Derived from Hemp Bast Fiber. *Fuller. Nanotub. Carbon Nanostruct.* **2022**, *30*, 873–882. DOI: 10.1080/1536383X.2022.2033729.

[12] Kumar, P. G.; Kumaresan, V.; Velraj, R. Stability, Viscosity, Thermal Conductivity, and Electrical Conductivity Enhancement of Multi-Walled Carbon Nanotube Nanofluid Using Gum Arabic. *Fuller. Nanotub. Carbon Nanostruct.* **2017**, *25*, 230–240. DOI: 10.1080/1536383X.2017.1283615.

[13] Bembenek, M.; Kotsyubynsky, V.; Boychuk, V.; Rachiy, B.; Budzulyak, I.; Kowalski, Ł.; Ropyak, L. Effect of Synthesis Conditions on Capacitive Properties of Porous Carbon Derived from Hemp Bast Fiber. *Energies* **2022**, *15*, 8761. DOI: 10.3390/en15228761.

[14] Berezkin, V. I.; Kholodkevich, S. V.; Konstantinov, P. P. Hall Eff Ect in the Natural Glassy Carbon of Shungites. *Phys. Solid State* **1997**, *39*, 1590–1593. DOI: 10.1134/1.1129903.

[15] Kovalevski, V. V.; Prikhodko, A. V.; Buseck, P. R. Diamagnetism of Natural Fullerene-like Carbon. *Carbon* **2005**, *43*, 401–405. DOI: 10.1016/j.carbon.2004.09.030.

[16] Melezhik, V. A.; Filippov, M. M.; Romashkin, A. E. A Giant Paleoproterozoic Deposit of Shungite in NW Russia. *Ore Geol. Rev.* **2004**, *24*, 135–154. DOI: 10.1016/j.oregeorev.2003.08.003.

[17] Buseck, P. R.; Galdobina, L. P.; Kovalevski, V. V.; Rozhkova, N. N.; Valley, J. W.; Zaidenberg, A. Z. Shungites: The C-Rich Rocks of Karelia, Russia. *Can. Miner.* **1997**, *35*, 1363–1378.

[18] Kovalevski, V. V.; Buseck, P. R.; Cowley, J. M. Comparison of Carbon in Shungite Rocks to Other Natural Carbons: An X-Ray and TEM Study. *Carbon* **2001**, *39*, 243–256. DOI: 10.1016/S0008-6223(00)00120-2.

[19] Golubev, Y. A.; Rozhkova, N. N.; Kabachkov, E. N.; Shul'ga, Y. M.; Natkaniec-Hołderna, K.; Natkaniec, I.; Antonets, I. V.; Makeev, B. A.; Popova, N. A.; Popova, V. A.; Sheka, E. F. sp^2 Amorphous Carbons in View of Multianalytical Consideration: Normal, Expected and New. *J. Non-Crystal. Solids* **2019**, *524*, 119608. DOI: 10.1016/j.jnoncrysol.2019.119608.

[20] Lyn'kov, L. M.; Borbot'ko, T. V.; Krishtopova, E. A. Radio-Absorbing Properties of Nickel-Containing Shungite Powder. *Tech. Phys. Lett.* **2009**, *35*, 410–411. DOI: 10.1134/S1063785009050071.

[21] Antonets, I. V.; Golubev, E. A.; Shavrov, V. G.; Shcheglov, V. I. Dynamic Microwave Conductivity of Graphene-Based Shungite. *Tech. Phys. Lett.* **2018**, *44*, 371–373. DOI: 10.1134/S1063785018050036.

[22] Golubev, Y. A.; Antonets, I. V.; Shcheglov, V. I. Static and Dynamic Conductivity of Nanostructured Carbonaceous Shungite Geomaterials. *Mater. Chem. Phys.* **2019**, *226*, 195–203. DOI: 10.1016/j.matchemphys.2019.01.033.

[23] Sheka, E. F.; Rozhkova, N. N. Shungite as Loosely Packed Fractal Nets of Grapheme Based Quantum Dots. *Int. J. Smart Nano Mater.* **2014**, *5*, 1–16. DOI: 10.1080/19475411.2014.885913.

[24] Sheka, E. F.; Golubev, E. A. Technical Graphene (Reduced Graphene Oxide) and Its Natural Analog (Shungite). *Tech. Phys.* **2016**, *61*, 1032–1038. DOI: 10.1134/S1063784216070239.

[25] Antonets, I. V.; Golubev, E. A.; Kotov, L. N.; Kalinin, Y. E.; Sitnikov, A. V. Nanostructure and Electrical Conductivity of Amorphous Granulated $(Co_{45}Fe_{45}Zr_{10})_x(Al_2O_3)_{1-x}$ Composite Films. *Tech. Phys.* **2016**, *61*, 416–423. DOI: 10.1134/S1063784216030038.

[26] Antonets, I. V.; Kotov, L. N.; Kirpicheva, O. A.; Golubev, E. A.; Kalinin, Y. E.; Sitnikov, A. V.; Shavrov, V. G.; Shcheglov, V. I. Static and Dynamic Conduction of Amorphous Nanogranulated Metal–Dielectric Composites. *J. Commun. Technol. Electron.* **2015**, *60*, 904–914. DOI: 10.7868/S0033849415070013.

[27] Antonets, I. V.; Golubev, E. A.; Shavrov, V. G.; Shcheglov, V. I. Representation of the Specific Conductivity of Graphene-Containing Shungite Based on the Current Tube Model. *J. Radio Electron.* **2020**, *2020*, 1–39. DOI: 10.30898/1684-1719.2020.3.7.

[28] Antonets, I. V.; Golubev, Y. A.; Shcheglov, V. I. Influence of Graphene Stacks on the Structure and Conductivity of Shungite Carbon. *IOP Conf. Ser. Mater. Sci. Eng.* **2021**, *1047*, 012162. DOI: 10.1088/1757-899X/1047/1/012162.

[29] Morozov, S. V.; Novoselov, K. S.; Geim, A. K. Electronic Transport in Grapheme. *Phys.-Usp.* **2008**, *51*, 744–748. DOI: 10.1070/PU2008v051n07ABEH006575.

[30] Hill, E. W.; Geim, A. K.; Novoselov, K.; Schedin, F.; Blake, P. Graphene Spin Valve Devices. *IEEE Trans. Magn.* **2006**, *42*, 2694–2696. DOI: 10.1109/TMAG.2006.878852.

[31] Golubev, E. A. Electrophysical Properties and Structural Features of Shungite (Natural Nanostructured Carbon). *Phys. Solid State* **2013**, *55*, 1078–1086. DOI: 10.1134/S1063783413050107.

[32] Shavrov, V. G.; Shcheglov, V. I. *Ferromagnetic Resonance under Conditions of Orientational Transition*; Fizmatlit: Moscow, **2018**.